First published October 26, 2011; doi:10.1152/ajpregu.00127.2011.

Increased NHE3 abundance and transport activity in renal proximal tubule of rats with heart failure

Bruna H. Inoue,[1] Leonardo dos Santos,[1,2] Thaissa D. Pessoa,[3] Ednei L. Antonio,[4] Bruna P. M. Pacheco,[1] Fernanda A. Savignano,[1] Luciene R. Carraro-Lacroix,[3] Paulo J. F. Tucci,[4] Gerhard Malnic,[3] and Adriana C. C. Girardi[1]

[1]*Heart Institute (InCor), University of São Paulo Medical School;* [2]*Department of Physiological Sciences, Federal University of Espírito Santo, Vitória, ES;* [3]*Department of Physiology and Biophysics, Institute of Biomedical Sciences, University of São Paulo; and* [4]*Department of Physiology, Federal University of São Paulo, São Paulo, Brazil.*

Submitted 14 March 2011; accepted in final form 19 October 2011

Inoue BH, dos Santos L, Pessoa TD, Antonio EL, Pacheco BPM, Savignano FA, Carraro-Lacroix LR, Tucci PJF, Malnic G, Girardi ACC. Increased NHE3 abundance and transport activity in renal proximal tubule of rats with heart failure. *Am J Physiol Regul Integr Comp Physiol* 302: R166–R174, 2012. First published October 26, 2011; doi:10.1152/ajpregu.00127.2011.—Heart failure (HF) is associated with a reduced effective circulating volume that drives sodium and water retention and extracellular volume expansion. We therefore hypothesized that Na^+/H^+ exchanger isoform 3 (NHE3), the major apical transcellular pathway for sodium reabsorption in the proximal tubule, is upregulated in an experimental model of HF. HF was induced in male rats by left ventricle radiofrequency ablation. Sham-operated rats (sham) were used as controls. At 6 wk after surgery, HF rats exhibited cardiac dysfunction with a dramatic increase in left ventricular end-diastolic pressure. By means of stationary in vivo microperfusion and pH-dependent sodium uptake, we demonstrated that NHE3 transport activity was significantly higher in the proximal tubule of HF compared with sham rats. Increased NHE3 activity was paralleled by increased renal cortical NHE3 expression at both protein and mRNA levels. In addition, the baseline PKA-dependent NHE3 phosphorylation at serine 552 was reduced in renal cortical membranes of rats with HF. Collectively, these results suggest that NHE3 is upregulated in the proximal tubule of HF rats by transcriptional, translational, and posttranslational mechanisms. Enhanced NHE3-mediated sodium reabsorption in the proximal tubule may contribute to extracellular volume expansion and edema, the hallmark feature of HF. Moreover, our study emphasizes the importance of undertaking a cardiorenal approach to contain progression of cardiac disease.

myocardial injury; renal function; volume homeostasis; radiofrequency ablation.

HEART FAILURE (HF) is a multifaceted clinical syndrome characterized by reduced cardiac output and/or diastolic dysfunction associated with venous and capillary congestion. These initial alterations in cardiac function are accompanied by a progressive series of systemic abnormalities at both functional and structural levels. A number of physiological mechanisms are triggered in the face of impaired cardiovascular hemodynamics and sustained loss of myocardial contractility caused by heart disease. Many of these mechanisms are adaptive on a short-term basis but are often maladaptive over the long term. Underfilling of the arterial system, a major hemodynamic abnormality in HF evokes a number of neurohumoral responses to maintain sufficient blood flow delivery to peripheral organs and thereby compensate for the progressively declining cardiac performance (7, 8). Stimulation of these neurohumoral mechanisms, which include activation of the sympathetic and renin-angiotensin-aldosterone systems (RAAS) and enhanced vasopressin release, may, in fact, further aggravate HF through increased cardiac load and excessive sodium and water retention by the kidneys (16, 17, 21, 38, 39).

The apical entry of sodium constitutes the rate-limiting step in transepithelial sodium and fluid transport. Hence, any changes in either the number and/or the intrinsic activity of the proteins mediating this entry can affect the rate of renal tubular reabsorption (30). Recent studies provide compelling evidence that increased protein abundance of the predominant apical sodium transporters may play an important role in the pathogenesis of sodium and water retention in HF. It has been demonstrated by several investigators that the protein abundance of the Na^+-K^+-$2Cl^-$ cotransporter NKCC2 is increased in the thick ascending limb of rats with HF induced by ligation of the left anterior descending coronary artery (LAD) (28, 31, 43, 48). Most recently, Lütken et al. (28) have shown that LAD-induced HF is associated with increased protein expression of Na^+/H^+ exchanger isoform 3 (NHE3) in renal cortex and outer medulla and altered expression of the epithelial sodium channel (ENaC) subunits. Nonetheless, to the best of our knowledge, there are no reports to date that have directly demonstrated that the activity of any of the major apical sodium transport proteins within the nephron is increased in HF.

The proximal tubule reabsorbs approximately two-thirds of the filtered sodium. NHE3-mediated Na^+/H^+ exchange is the principal apical membrane mechanism for sodium reabsorption in this nephron segment (4, 40, 51, 52). Considering the quantitative importance of NHE3 in mediating sodium reabsorption in the renal proximal tubule, changes in the activity of this exchanger for extended periods can have a great impact on extracellular volume homeostasis. We therefore hypothesized that NHE3 activity is increased in the renal proximal tubule of HF rats, potentially contributing to sodium retention, extracellular volume expansion, and ultimately to edema. In the present study, we made use of both in vivo and ex vivo approaches to measure NHE3 activity in an experimental model of HF, recently developed by Antonio et al. (2) in which rats are subjected to myocardial injury by means of radiofrequency ablation of the left ventricle. The molecular mechanisms un-

Address for reprint requests and other correspondence: A. C. C. Girardi, Laboratory of Genetics and Molecular Cardiology, Heart Institute, Univ. of São Paulo Medical School, Avenida Dr. Enéas de Carvalho Aguiar, 44, 10° Andar, Bloco II, 05403-900 São Paulo, SP, Brazil (e-mail: adriana.girardi@incor.usp.br).

derlying altered regulation of NHE3 in the renal proximal tubule of rats with HF were also explored.

MATERIALS AND METHODS

Animal protocols and surgical procedures. All animal work was conducted in accordance with the ethical principles in animal research of the Brazilian College of Animal Experimentation and was approved by the institutional animal care and use committee. Experimental HF was induced in male Wistar rats (200–250 g) by left ventricular (LV) myocardial injury after radiofrequency catheter ablation (2). In brief, rats were anesthetized with halothane and a left thoracotomy was performed at the fourth intercostal space. The left pericardium was opened, and the tip of a custom-made catheter was placed on the LV anterolateral wall, perpendicular to the tissue, under constant manual pressure. LV lesions were created by delivering high-frequency currents (1,000 KHz, 12 watts, during 10 s) generated by a conventional radiofrequency generator (model TEB RF10; Tecnologia Eletrônica Brasileira, São Paulo, Brazil). The damaged area was immediately visualized by the presence of a clear, white disk-shaped region of coagulation necrosis. Thereafter, the heart was quickly returned to the thorax, and a suture was used to close the chest. Sham-operated rats underwent left thoracotomy and were mockingly ablated. All the following experimental procedures were performed 6 wk after myocardial injury for HF induction or sham operation.

Renal function studies. Rats were anesthetized with ketamine-xylazine-acepromazine (64.9, 3.20, and 0.78 mg/kg sc, respectively) and placed on a heated surgical table to maintain body temperature. After tracheostomy, polyethylene (PE) catheters were inserted into the jugular vein and the urinary bladder for inulin infusion and urine collection, respectively. To control mean arterial pressure (MAP) and allow blood sampling, a PE-60 catheter was inserted into the right carotid artery. Glomerular filtration rate was determined by measuring the clearance of inulin as follows. First, a loading dose of inulin (100 mg/kg in 0.9% saline) was administered and, subsequently, continuous infusions of inulin (10 mg/kg in 0.9% saline) were made at 0.04 ml/min. Three consecutive 30-min periods of urine collection were performed. Blood samples were obtained at the beginning and at the end of the experiment. Plasma and urine sodium concentrations were measured by flame photometry (model B262; Micronal, São Paulo, Brazil), and inulin was determined by using the anthrone method (12).

Hemodynamic studies. After renal function assessment, invasive hemodynamic studies were performed to evaluate cardiac performance. Rats were anesthetized using an intraperitoneal injection of ketamine (50 mg/kg) and xylazine (10 mg/kg) and placed on a heated rodent operating table (37°C) under oxygen-enriched mechanical ventilation. A MicroTip pressure-volume catheter (model 1.4 French SPR 839; Millar Instruments, Houston, TX) was then inserted into the right carotid artery and positioned immediately above the aortic valves to monitor aortic blood pressure. After 5 min of arterial blood pressure recording, the catheter was advanced into the LV cavity for simultaneous and continuous pressure and volume measurements. Volume calibration was accomplished by using a linear volume-conductance regression of the absolute blood volume (4 cylindrical chambers containing a specified volume of fresh heparinized rat blood) versus the correspondent signal acquired by the conductance catheter. Data were acquired for computer analysis (PVAN Software, Millar Instruments) using LabChart 7 Software System (PowerLab, ADInstruments, Bella Vista, NSW, Australia). The following data were obtained: heart rate (HR), MAP, LV end-systolic and end-diastolic pressures (LVEDP), maximal rate of LV pressure rise ($+dP/dt_{max}$) and decline ($-dP/dt_{max}$), time constant of LV pressure decay (Tau), stroke volume, cardiac output, and stroke work. Tau was calculated as the time constant of monoexponential pressure decay during the isovolumetric relaxation: $P(t) = A + B \exp(-t/\text{Tau})$. The total peripheral resistance index (TPRI) was calculated (TPRI = MAP/cardiac output). Only rats with LVEDP $>$ 15 mmHg were included in the HF group.

Stationary in vivo microperfusion. Experiments were carried out essentially as described previously (10), including anesthesia and surgical preparation for in vivo micropuncture. Proximal tubules were punctured by means of a double-barreled micropipette, one barrel being used to inject FDC green-colored Ringer perfusion solution and the other to inject Sudan-black colored castor oil. To measure luminal pH, proximal tubules were impaled by a double-barreled asymmetric microelectrode, the larger barrel containing the H^+-ion sensitive ion-exchange resin and the smaller barrel containing the reference solution (1 M KCl) colored by FDC green. By continuously measuring the luminal pH toward the steady-state level, the rate of tubular acidification, representing bicarbonate reabsorption, was evaluated in a solution, isolated, and blocked by oil. Thereby, luminal HCO_3^- activity, starting at 25 mM (perfusion solution) was progressively reduced to a stationary level by H^+ secretion. The voltage between the microelectrode barrels, representing luminal H^+ activity, was continuously recorded by means of a microcomputer equipped with an AD converter (Lynx, São Paulo, Brazil). Luminal bicarbonate was calculated from luminal pH and arterial blood P_{CO_2}, and the rate of tubular acidification was expressed as the half time of the exponential reduction of the injected HCO_3^- concentration to its stationary level.

Postmortem analysis. At the end of the experimental procedures, rats were killed by decapitation, and their hearts, lungs, and kidneys were quickly removed. Heart injury in HF rats was evaluated as follows. Right and left ventricle, including the interventricular septum were separately weighed, fixed in 10% formalin, and embedded in paraffin. Sections (5 μm) of paraffin-embedded tissue were mounted onto slides and stained with Picrossirius red for measurement of collagen scar and LV cavity perimeter. The slides were next scanned and digitally analyzed (Image Tool 3.0; University of Texas Health Science Center San Antonio, San Antonio, TX). Myocardial lesion was quantified by the percentage of LV perimeter containing scar tissue. Lung weights (indexed by body weight and tibia length) were taken as a marker of pulmonary congestion. Kidney cortices were cut off and used for the preparation of either renal cortical membrane vesicles or for RNA isolation.

Isolation of renal cortical membranes. Renal cortical membranes were prepared by differential centrifugation of renal cortical homogenates from individual animals as described previously (11). Protein concentration was determined by the method of Lowry (27).

Microvillus membrane preparation. Microvillus membrane vesicles (MMV) were isolated from renal cortices of individual animals as described previously (3). Membranes were isolated and stored in 200 mM mannitol, 80 mM HEPES, 41 mM KOH, 1 μM pepstatin, 1 μM leupeptin, 230 μM PMSF, pH 7.5 at −80°C. MMV preparations used in this study were 11- to 14-fold enriched in specific activity of the brush-border membrane marker enzyme γ-glutamyltranspeptidase relative to kidney homogenates. Protein concentration was determined by the method of Lowry (27).

Radioactive sodium uptake. Renal cortical membranes were washed and equilibrated for 2 h at room temperature in 254 mM mannitol, 35 mM KOH, 68 mM HEPES, 50 mM MES, pH 6.0. The membranes were then centrifuged and resuspended in the same solution at a final protein concentration of 10 μg/μl. The uptake of ^{22}Na was then assayed after mixing 10 μl of the renal cortical membrane suspension with 90 μl of a hot solution containing 0.1 μCi of ^{22}Na, 300 mM mannitol, 42 mM KOH, 80 mM HEPES, pH 7.5. The uptake reaction was stopped after 10 s by the addition of 3 ml ice-cold solution (stop solution) containing 100 mM KCl, 42 mM KOH, 80 mM HEPES, pH 7.5. Renal cortical membrane vesicles were collected on 0.65-μm Millipore filters. After the filters were washed with an additional 9.0 ml of stop solution, ^{22}Na radioactivity was measured using a liquid scintillation counter. Some experiments were performed in the presence of 10 μM (S3226) to inhibit NHE3 activity.

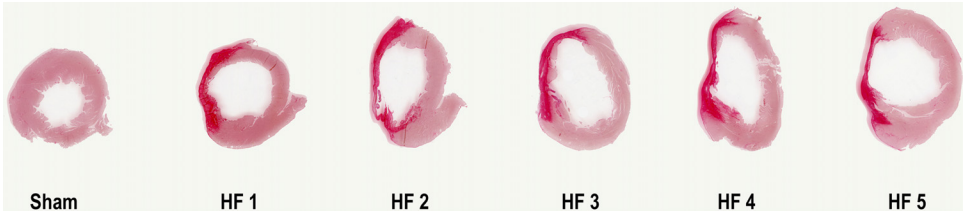

Fig. 1. Representative hearts of sham-operated and rats that underwent left ventricle (LV) radiofrequency ablation [heart failure (HF)]. Sections (5 μm) of paraffin-embedded cardiac tissue were mounted onto slides and stained with Picrossirius red for measurement of collagen scar and LV cavity perimeter.

SDS-PAGE and immunoblotting. Protein samples were subjected to SDS-PAGE, transferred to polyvinylidene fluoride (PVDF) membranes (Immobilon-P; Millipore, Bedford, MA) and prepared for immunoblotting as previously described (10). The PVDF membranes were incubated with Blotto (5% nonfat dry milk and 0.1% Tween 20 in PBS, pH 7.4) for 1 h at room temperature to block nonspecific binding and were subsequently incubated overnight at 4°C with the primary antibody in Blotto at the following concentrations: 1:1,000 anti-PS552 (24), 1:1,000 anti-NHE3 (5), or 1:50,000 anti-actin. The membranes were then washed five times with Blotto and incubated for 1 h with horseradish peroxidase-conjugated immunoglobulin secondary antibody (1:2,000). Membranes were again washed five times with Blotto and then rinsed in PBS. Bound antibody was detected using an enhanced chemiluminescence system (GE Healthcare) according to the manufacturer's protocols. The visualized bands were digitized using the ImageScanner III (GE HealthCare) and quantified using Image Software (Scion, Federick, MD).

RNA isolation and real-time RT-PCR reaction. Total RNA was isolated by the acid guanidinium thiocyanate phenol-chloroform method and cDNA synthesis was performed with random hexamers (High Capacity cDNA Archive kit-PE; Applied Biosystems) following the manufacturer's guidelines. Fifteen nanograms of cDNA were used for real-time RT-PCR reaction (SYBR Green PCR Master Mix-PE; Applied Biosystems) in an ABI Prism 7700 Sequence Detection System (Applied Biosystems). All samples were assayed in triplicate. The comparative threshold cycle method was used for data analyses. The following oligonucleotide primers were used: NHE3: 5′-ACTGCTTAATGACGCGGTGACTGT-3′ (forward) and 5′-AAAGACGAAGCCAGGCTCGATGAT-3′ (reverse), and 28S: 5′-TCATCAGACCCCAGAAAAGG-3′ (forward) and 5′-GATTCG-GCAGGTGAGTTG-3′ (reverse).

Statistical analyses. All results are reported as means ± SE with n indicating the number of observations. Comparisons between two groups were performed using unpaired t-tests. If more than two groups were compared, statistical significance was determined by ANOVA followed by Tukey's post hoc test. Results were considered significant when $P < 0.05$.

RESULTS

Experimental model, biometric, and cardiac parameters. Herein, we used an experimental model of HF in which rats were subjected to myocardial injury by means of LV radiofrequency ablation (2). The major advantages of this model are the very consistent size of myocardial injury and low immediate (24 h) mortality rate. Accordingly, only 1 out of 22 rats died 24 h after being subjected to the procedure. Additionally, 6 wk after LV radioablation, we verified by standard histological analysis with Picrossirius red staining that LV radiofrequency ablation gave rise to a myocardial injury that was very reproducible in terms of both site (Fig. 1) and size (35.4 ± 2.6% of LV).

Table 1 summarizes the biometric parameters found in HF and sham-operated rats. Compared with sham animals, rats with HF did not display significant changes in body or absolute heart weight. However, when normalized by tibial length or body wt, relative heart weight was significantly increased in HF animals. In addition, the relative weight of the wet right lung was also significantly increased in HF animals compared with the sham group, suggestive of pulmonary congestion secondary to cardiac decompensation.

Figure 2 shows representative steady-state pressure-volume loops (P-V loops; Fig. 2*A*) and the pressure signal and dP/dt (Fig. 2*B*) obtained from individual HF and sham rats 6 wk after LV radioablation or sham operation, illustrating the typical hemodynamic changes that occur in HF. The rightward shift of the P-V loops and the decrease of the area within the P-V loop curves and of +dP/dt in HF rats indicates a decrease in cardiac performance. As shown in Table 2, HF was associated with a significant decrease of the maximal slope of the systolic pressure increment (+dP/dt_{max}), cardiac output, and stroke work when compared with sham animals, with no significant changes in HR, LV systolic pressure, and MAP, overall suggestive of relative LV systolic impairment. Furthermore, maximal rate of LV pressure decline (−dP/dt_{max}) was depressed (Fig. 2*B* and Table 2) and LVEDP (Fig. 2*B* and Table 2) and the time constant of isovolumetric relaxation (Tau) (Table 2) were increased in HF animals, indicating diastolic dysfunction. The TPRI was also significantly increased in HF rats. In line with previous findings (2), our data indicate that this experimental model of post-myocardial injury HF displays many abnormalities of cardiac function that resembles the human syndrome.

Renal function evaluation. Renal function studies were carried out 6 wk after myocardial injury or sham operation. As shown in Table 3, urinary flow, glomerular filtration rate, urinary excretion of sodium, and fractional excretion of sodium were not statistically different between HF and sham, although a tendency to a decrease in rats with HF was observed. Daily sodium and water intake were also measured in sham and HF

Table 1. *Organ weights for sham-operated and heart failure rats*

	Sham	Heart Failure
No.	7	9
Body weight, g	441 ± 12	446 ± 17
Tibia length, mm	40.4 ± 0.4	40.7 ± 0.5
Heart wt, mg	1,230 ± 39	1,336 ± 33
Heart wt/body wt, mg/g	2.79 ± 0.03	3.03 ± 0.06*
Heart wt/tibia, mg/mm	29.6 ± 1.2	33.6 ± 0.5*
Right lung, mg	1,170 ± 71	1,428 ± 128
Right lung/body wt, mg/g	2.55 ± 0.13	4.11 ± 0.49*
Right lung/tibia, mg/mm	27.7 ± 1.4	37.2 ± 3.7*

Values are means ± SE; *$P < 0.05$ vs. sham, unpaired Student's t-test.

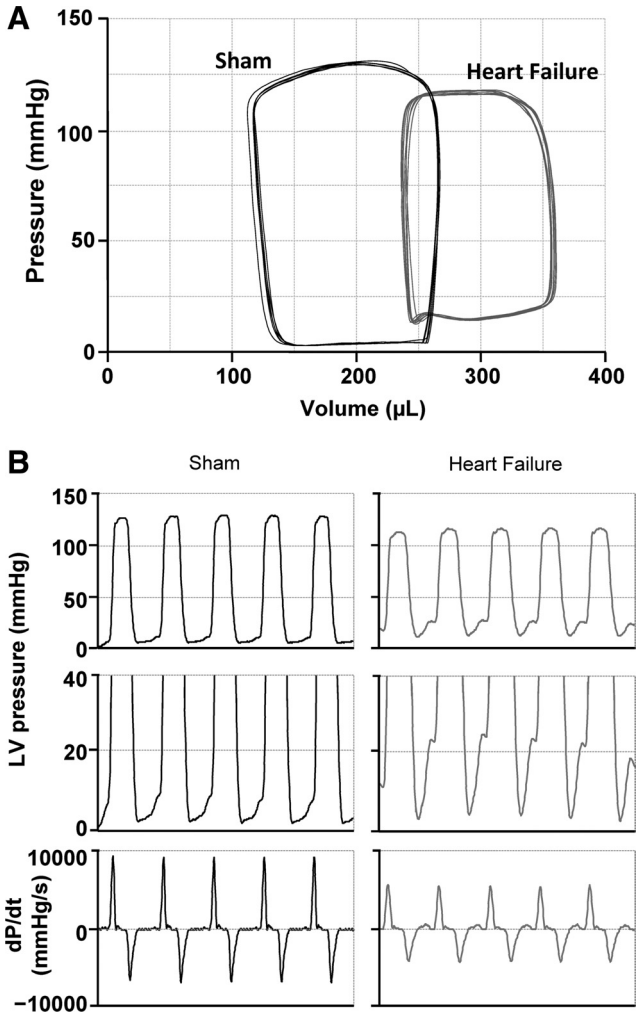

Fig. 2. LV pressure-volume relationship in sham and HF rats. Representative pressure-volume loops in *A* and intraventricular pressure and dP/d*t* signals in *B* were obtained from sham and HF rats 6 wk after LV radiofrequency ablation or sham operation. In *A*, note that impaired ability of the heart to fill with blood and then to eject it shifts the end-diastolic pressure and volume relationship right and downward.

rats for three consecutive days prior to the experiments of renal function evaluation. Throughout this period, the daily average consumption of water (67.8 ± 4.4 vs. 69.4 ± 1.9 ml/kg, $P < 0.05$ vs. sham) and sodium (5.93 ± 0.41 vs. 5.97 ± 0.37 meq/kg, $P < 0.05$ vs. sham) were similar between these two groups of animals.

NHE3-mediated Na^+/H^+ exchange in renal proximal tubule. A major fraction of proximal tubular bicarbonate reabsorption is mediated by proton secretion through NHE3 (40, 52). We therefore evaluated whether the in vivo NHE3 transport activity was altered in HF rats compared with sham by measuring the rate of bicarbonate reabsorption ($J_{HCO_3^-}$) in the native proximal tubules of these animals. To this end, stationary in vivo microperfusion experiments were conducted in individual proximal convoluted tubules from HF ($n = 5$) and sham-operated rats ($n = 4$). As indicated in Fig. 3*A*, $J_{HCO_3^-}$ was significantly increased (43 ± 6%) in HF rats compared with sham (2.71 ± 0.33 vs. 1.90 ± 0.11 nmol·cm^2·s^{-1}; $P < 0.05$).

Table 2. *Hemodynamic parameters in sham-operated and heart failure rats measured by the Millar pressure-volume conductance catheter system*

	Sham	Heart Failure
No.	7	9
Heart rate, beats/min	253 ± 15	260 ± 11
MAP, mmHg	104 ± 6	104 ± 4
LVSP, mmHg	125 ± 9	110 ± 6
LVEDP, mmHg	4.8 ± 0.9	23.9 ± 2.6*
CO, ml/min	32.2 ± 2.2	24.2 ± 1.0*
SW, mmHg/ml	15.4 ± 1.4	9.9 ± 0.8*
$+dP/dt_{max}$, mmHg/s	8,909 ± 169	7,092 ± 338*
$-dP/dt_{max}$, mmHg/s	−8,205 ± 948	−5,444 ± 349*
Tau, ms	11.5 ± 0.6	16.9 ± 0.8*
TPR, mmHg·ml^{-1}·min^{-1}	3.2 ± 0.2	4.4 ± 0.2*

Values are means ± SE. MAP, mean arterial pressure; LVSP, left ventricular (LV) systolic pressure; LVEDP, LV end-diastolic pressure; CO, cardiac output; SW, stroke work; $+dP/dt_{max}$ and $-dP/dt_{max}$, maximal rate of LV pressure increment and decrement, respectively; Tau, time constant of LV pressure decay; TPR, total peripheral resistance. *$P < 0.05$ vs. sham; unpaired Student's *t*-test.

We next evaluated NHE3 activity by measuring the proton dependent uptake of ^{22}Na in renal cortical membrane vesicles isolated from HF ($n = 4$) and sham animals ($n = 4$) (Fig. 3*B*). In agreement with the micropuncture results, NHE3-mediated-^{22}Na uptake (= S3226-inhibitable ^{22}Na uptake) was higher in HF rats than in sham (58 ± 3%). No significant differences were observed between sham and HF rats in the component of ^{22}Na uptake that was insensitive to the specific inhibitor of NHE3 activity, S3226 (41). Taken together, these results suggest that altered renal handling of sodium in HF is at least partially attributed to enhanced NHE3-mediated sodium reabsorption in the renal proximal tubule.

NHE3 protein and mRNA expression in total renal cortex. To investigate whether upregulation of NHE3 activity in HF was associated with increases of NHE3-protein abundance and/or mRNA levels, we carried out immunoblot and real-time RT-PCR analyses, respectively (Fig. 4). In accordance with results of a previous study in LAD-induced HF rats (28), we found that NHE3 protein abundance was 68 ± 8% higher in renal cortex of myocardial-injured HF rats compared with sham (Fig. 4*A*). Next, we determined whether the increase in NHE3 protein amount was accompanied by similar increases in the abundance of NHE3-mRNA in renal cortex. The data presented in Fig. 4*B* reveal that NHE3-mRNA expression relative to that of 28S ribosomal RNA was significantly higher in HF rats than in sham (145 ± 18%). Collectively, these

Table 3. *Renal function in sham-operated and heart failure rats*

	Sham	Heart Failure
No.	8	10
Urine output, μl·min^{-1}·kg^{-1}	32.9 ± 3.3	28.8 ± 3.67
GFR, ml·min^{-1}·kg^{-1}	4.37 ± 0.15	3.72 ± 0.29
Urinary Na^+, μmol·min^{-1}·kg^{-1}	1.90 ± 0.44	1.27 ± 0.16
FE Na^+, %	0.31 ± 0.05	0.22 ± 0.03

Values are means ± SE. Renal function was measured in anesthetized rats as described in MATERIALS AND METHODS. Urine output was measured gravimetrically. Inulin clearance was used to measure glomerular filtration rate (GFR). Renal functional data were corrected by body weight and expressed per kilogram body weight. FE, fractional excretion.

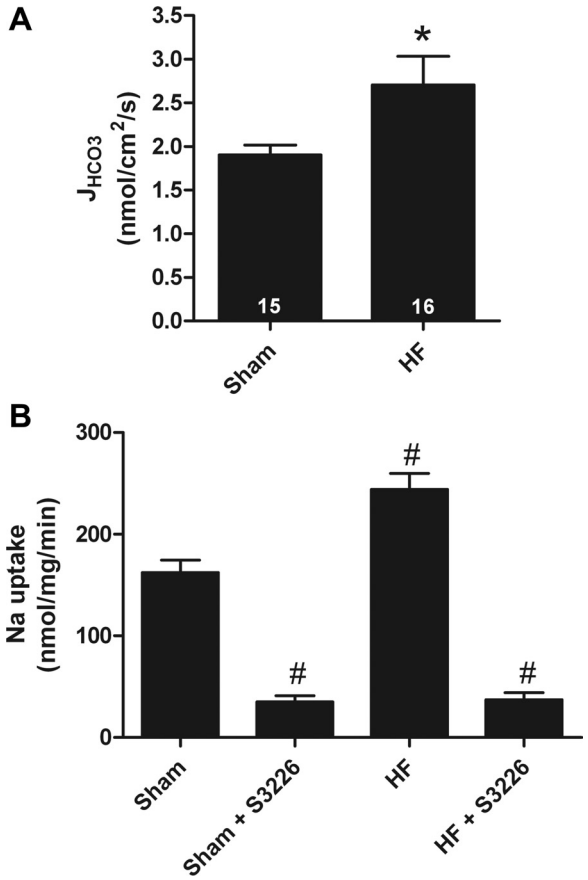

Fig. 3. Na^+/H^+ exchange (NHE3) mediated is increased in renal proximal tubule of HF rats. NHE3 activity was measured in vivo by stationary microperfusion (*A*) and ex vivo by proton gradient-dependent sodium uptake (*B*). *A*: rate of bicarbonate reabsorption ($J_{HCO_3^-}$) in the native proximal tubule of sham-operated (sham, $n = 4$) and HF rats ($n = 5$). The number of perfused tubules is indicated in the bars. Data are expressed as means ± SE. $^*P < 0.05$ vs. sham. *B*: NHE3-mediated proton-dependent uptake of ^{22}Na into renal cortical membrane vesicles of sham-operated and HF rats. Experiments were performed in the presence or absence of the specific NHE3 inhibitor S3226 (10 μM). Each assay was performed in triplicate, and the mean value of 4 animals from each group was calculated. $^{\#}P < 0.001$ vs. sham.

findings suggest that the upregulation of proximal tubule NHE3 activity in HF rats is, at least in part, dependent on changes in NHE3 protein abundance and NHE3-mRNA expression levels.

Levels of NHE3 phosphorylated at the PKA consensus site serine 552. One of the best-studied regulatory mechanisms affecting NHE3 activity is the inhibition resulting from agonists that activate cAMP-dependent protein kinase (PKA) (15, 24, 25). PKA directly phosphorylates NHE3 at serines 552 and 605, and it has been established that the residue 552 of NHE3 is phosphorylated to a much greater extent than the residue 605 at baseline in vivo (24). To determine whether altered phosphorylation of NHE3 may contribute to the increased activity of the exchanger in the renal proximal tubule of HF rats, we examined the levels of phosphorylated NHE3 in renal cortical membranes by means of immunoblotting. Experiments were carried out using a phosphospecific monoclonal antibody that recognizes NHE3 only when it is phosphorylated at serine 552 (24). As seen in Fig. 5, the relative ratio of NHE3-PS552/NHE3 total was significantly lower in renal cortical membranes isolated from HF compared with sham rats (−64 ± 4%).

The NHE3 phosphorylation status was also evaluated within the proximal tubule brush-border microvilli in HF and sham rats. As seen in Fig. 6, total NHE3 expression in MMV isolated from HF rats was higher (77 ± 10%, $P < 0.001$), and the PS552-NHE3-to-NHE3 ratio was lower than in sham (−60 ± 21%, $P < 0.05$). These results suggest that enhanced sodium reabsorption in the renal proximal tubule of HF rats is partially mediated through reduced baseline PKA-dependent phosphorylation of NHE3 at serine 552.

DISCUSSION

More than 50 years ago, Stead and Warren (44) noted that the most important causes of edema in HF are salt and water retention by the kidneys rather than the high venous pressure caused by impaired pumping of blood out of venous system. The potential causes of altered renal handling of salt and water may involve a decrease in glomerular filtration rate, an increase in tubular reabsorption of sodium, or both. In the present work, we demonstrate that the activity of the major proximal tubule sodium transporter NHE3 is increased in an experimental model of myocardial injury-induced HF. Higher NHE3 activity in the proximal tubule of HF rats is accompanied by enhanced renal cortical NHE3 expression at both mRNA and protein levels. In addition, the baseline PKA-dependent NHE3 phosphorylation at serine 552 is reduced in cortical membranes of rats with HF.

Numerous observations underscore the crucial role of NHE3 on extracellular volume control. NHE3 is acutely and chronically regulated by the renin-angiotensin system (14, 20, 37, 49, 54), sympathetic nervous system (55), as well as by an intrarenal dopamine natriuretic system (22, 29, 33). Moreover, NHE3 knockout mice are hypovolemic and exhibit reduced blood pressure (40). Furthermore, it has been previously demonstrated by other laboratories and ours that during the prehypertensive stage, NHE3 activity is increased in the renal proximal tubule of spontaneously hypertensive rats, possibly contributing to sodium retention and volume expansion in these animals (10, 26, 46). Here we show by both in vivo and ex vivo approaches that proximal tubule NHE3-mediated sodium reabsorption is increased in HF. Upregulation of NHE3 activity is accompanied by increases of NHE3 protein and mRNA expression. Of note, increased NHE3 protein expression have been previously observed in other experimental models of edematous disorders, including HF induced by ligation of the left anterior descending coronary artery (28) and cirrhosis (18). Despite upregulation of NHE3 function and expression, we did not find a statistically significant change of renal sodium handling after 6 wk of experimentally induced HF. Most likely, the animals might have experienced a positive sodium balance during the initial phase of heart failure and then reached a new steady state in which renal sodium output matches sodium intake.

NHE3 is phosphorylated on serine 552 under basal conditions by the adenylyl cyclase/cAMP-activated-protein kinase A (PKA) (24, 25) and the endogenous levels of phosphorylation is often affected as part of acute NHE3 regulation (15, 23, 24). Interestingly, baseline levels of NHE3 phosphorylation at this residue may also be associated with chronic regulation of

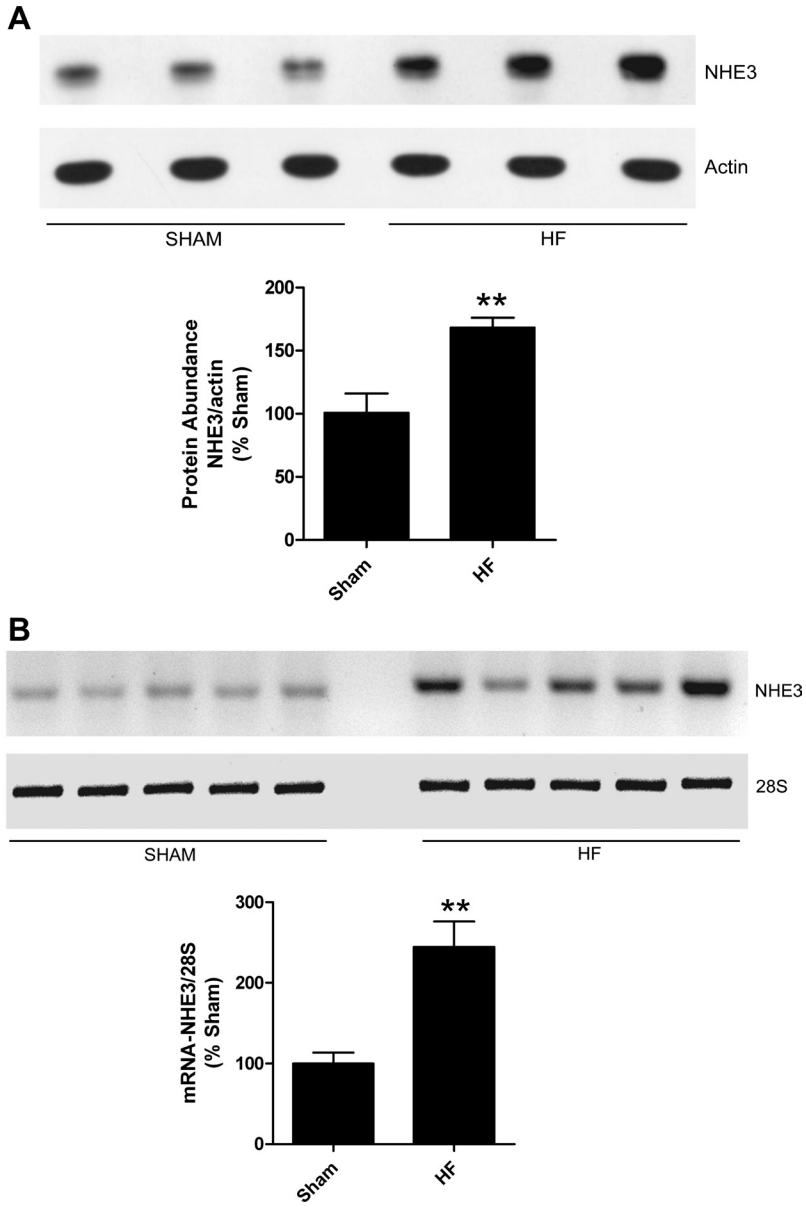

Fig. 4. NHE3 protein and mRNA expression are increased in renal proximal tubule of HF rats. *A, top*: representative immunoblot of NHE3 expression in renal cortex of SHAM and HF rats. Equivalent samples (15 μg of protein for NHE3 and 5 μg for actin) of renal cortical membranes isolated from sham-operated and HF rats were subjected to SDS-PAGE, transferred to PVDF membranes, and analyzed by immunoblotting. Membranes were incubated with monoclonal antibodies against NHE3 (1:1,000, clone 2B9; Millipore, Temecula, CA) and actin (1:50,000, clone JLA20; Merck, Darmstadt, Germany). *Bottom:* graph of the relative protein expression levels of NHE3 in renal cortical membranes. Values are means ± SE; $n = 4$/group, $^{**}P < 0.01$ vs. sham. *B, top*: RT-PCR analysis of NHE3 and 28S in renal cortex of sham and HF rats. The PCR products were analyzed by electrophoresis on agarose gel. *Bottom:* graph of relative mRNA-NHE3 expression levels in renal cortical membranes. NHE3-mRNA expression was quantified by real-time RT-PCR. Levels of NHE3-mRNA were normalized to those of internal control 28S ribosomal RNA (r28S-RNA). Values are means ± SE. $n = 5$/group, $^{**}P < 0.01$ vs. sham.

NHE3 activity. In this regard, we have recently demonstrated that NHE3 activity is differentially regulated before and after development of hypertension in spontaneously hypertensive rats and that these changes of NHE3 activity occur concurrently with changes of NHE3 phosphorylation status in the spontaneously hypertensive rat model. In this work, we show that the levels of NHE3 phosphorylation at the PKA consensus site serine 552 in the proximal tubule apical membrane of HF rats are lower than in sham animals. Thus, the molecular mechanisms mediating enhanced sodium reabsorption in the renal proximal tubule of HF rats also appear to involve post-translational covalent modification of NHE3. Moreover, decreased NHE3 phosphorylation at serine 552 is associated with an increase of NHE3 abundance in the brush-border microvilli, supporting the notion that phosphorylation of NHE3 at this specific PKA consensus site may play a role in subcellular trafficking of the transporter in vivo (23, 24). In congestive HF, volume expansion occurs in the venous side of the circulation, while the arterial underfilling due to reduced cardiac output is perceived as a plasma volume deficit by the arterial baroreceptors (7). Consequently, a series of neurohumoral adjustments is evoked that prevents the kidney to excrete accumulated salt and water. Among these neurohumoral responses are the activation of the renin-angiotensin-aldosterone (RAA) and the sympathetic nervous systems.

Both ANG II and norepinephrine have been shown to chronically increase NHE3 protein expression (42, 50, 54) and could be involved in upregulation of transporter expression in HF. Sonalker et al. (42) have demonstrated that chronic norepinephrine infusion resulted in a significant increase of NHE3 protein abundance in the rat renal cortex. Studies by several groups demonstrate that administration of ANG II increases NHE3 expression at both protein and mRNA levels in rat renal proximal tubule (14, 50) and cell culture models (34, 54). Additionally, LAD-induced HF rats treated with ANG II receptor antagonists display normalized levels of NHE3 expres-

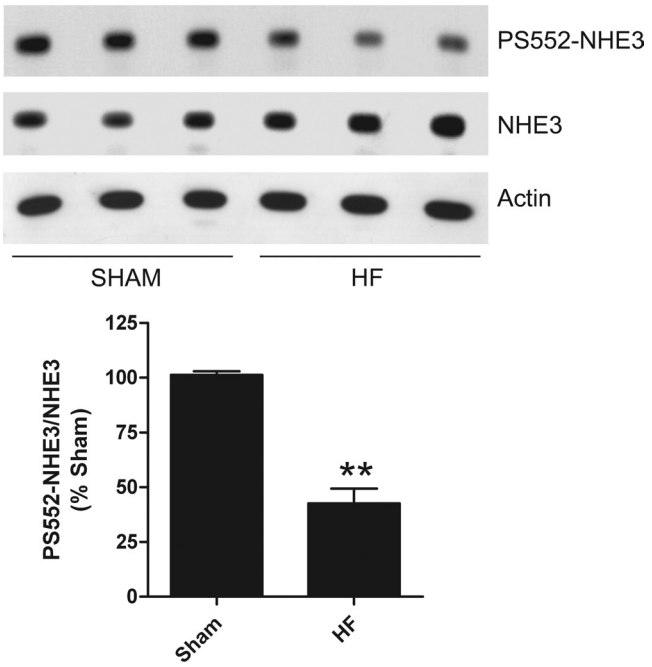

Fig. 5. Relative phosphorylation ratio of NHE3 at serine 552 (PS552-NHE3) is decreased in renal cortical membranes from HF rats. *Top*: representative immunoblot of phosphorylated and total NHE3 expression in renal cortex of sham and HF rats. Equivalent samples (15 μg of protein for NHE3 and 5 μg for PS552-NHE3 and actin) of renal cortical membranes isolated from sham-operated and HF rats were subjected to SDS-PAGE, transferred to PVDF membranes, and analyzed by immunoblotting. Membranes were incubated with monoclonal antibodies against phosphorylated NHE3 at serine 552 (1:1,000), total NHE3 (1:1,000), or anti-actin (1:50,000). *Bottom:* graph of the relative phosphorylation ratio of NHE3 at serine 552 in renal cortical membranes (PS552-NHE3/NHE3). Values are means ± SE. $n = 4$/group, $^{**}P < 0.01$ vs. sham.

sion (28) and renal sodium excretion (43), suggesting that ANG II influences renal sodium handling in cardiovascular disease at least, in part, via NHE3.

There is evidence that coupling of ANG II to the AT1 receptor inhibits cAMP accumulation and stimulates transcellular sodium transport in renal proximal tubule cells (45). β-Adrenoceptors also stimulate proximal tubule sodium reabsorption; however, these receptors are coupled to Gs proteins, which activate adenylyl cyclase to form cAMP. This paradox was explained by Hall et al (19) who demonstrated that β_2-receptors physically interact with the sodium proton exchanger regulatory factor (NHERF1), a protein that is required for PKA-mediated inhibition of NHE3. Stimulation of β_2-adrenoceptors by its ligands sequestrates NHERF and relieves the baseline inhibition of NHE3 by PKA. Thus, the decreased levels of endogenous NHE3 phosphorylation observed in the proximal tubule of HF rats might as well be mediated by activation of the RAAS and/or the sympathetic nervous system.

Both atrial and brain natriuretic peptides (ANP and BNP, respectively), originating in the myocardial cells and secreting into the plasma, play an important role in regulating extracellular fluid homeostasis and blood pressure by counterbalancing the RAAS and the sympathetic nervous system (13, 35, 53). Plasma levels of ANP and BNP have been shown to be increased in patients with HF and positively correlate with LV dysfunction (6, 35, 36, 47, 56). In fact, plasma concentrations of BNP have been widely used as a reliable prognostic indicator for HF patients in all stages of the disease (32). Notably, despite increases in the circulating levels of natriuretic peptides, renal sodium retention, volume expansion, and edema are continuously observed in patients and in experimental animal models of HF. Indeed, resistance to the natriuretic actions of ANP and BNP has been documented in HF subjects (1, 9). Numerous explanations for natriuretic peptide resistance in HF have been anticipated (7). Our results suggest that enhanced NHE3-mediated proximal tubular sodium reabsorption diminishes sodium delivery to the distal nephron site of natriuretic peptide action. Such decreased sodium load to the distal nephron may attenuate the natriuretic response to these peptides in HF patients.

Perspectives and Significance

The present study demonstrates that NHE3-mediated Na^+/H^+ exchange is significantly increased in the renal proximal tubule of an experimental model of post-myocardial injury HF. The molecular mechanisms underlying upregulation of NHE3 activity in HF seem to occur at transcriptional, translational, and posttranslational levels. These novel findings suggest that enhanced NHE3-mediated sodium reabsorption in the proximal tubule may contribute to extracellular volume expansion and ultimately to edema, one of the most important pathophysiological features of HF. Moreover, our study emphasizes the importance of undertaking a cardiorenal approach to contain

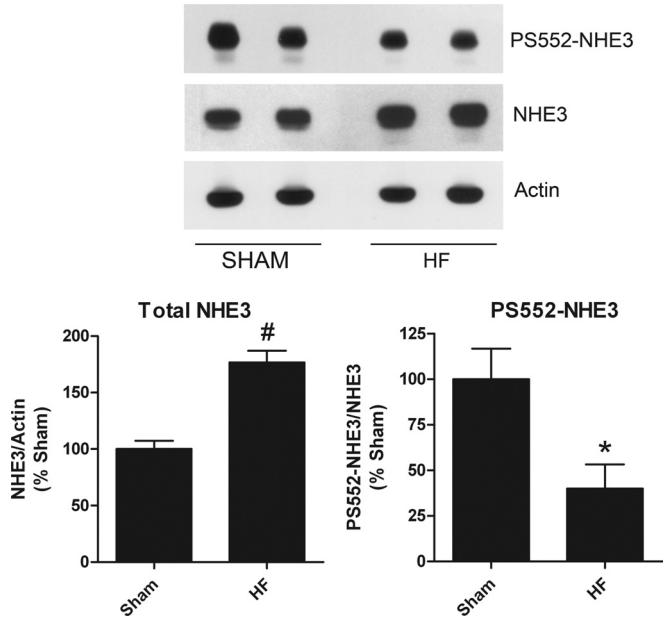

Fig. 6. NHE3 expression is increased and the relative phosphorylation ratio of NHE3 at serine 552 is decreased in microvillus membrane vesicles (MMV) from HF rats. *Top*: representative immunoblot of phosphorylated and total NHE3 expression in MMV of sham and HF rats. Equivalent samples (15 μg of protein for NHE3 and 5 μg for PS552-NHE3 and actin) of MMV isolated from sham-operated and HF rats were prepared for immunoblot analysis. The membranes were incubated with monoclonal antibodies against phosphorylated NHE3 at serine 552 [PS552-NHE3 (1:1,000)], total NHE3 (1:1,000), or anti-actin (1:50,000). *Bottom, left:* graph of relative expression levels of NHE3 in MMV. *Right:* graph of phosphorylation ratio of NHE3 at serine 552 to total NHE3 in MMV (PS552-NHE3/NHE3). Values are means ± SE. $n = 4$/group, $^{*}P < 0.05$ and $^{\#}P < 0.001$ vs. sham.

progression of cardiac disease. Improving the understanding of the kidney's adaptive and maladaptive responses to cardiac dysfunction may lead to the development of new therapeutic strategies.

GRANTS

This research was supported by Fundação de Amparo à Pesquisa do Estado de São Paulo, Conselho Nacional de Desenvolvimento Cientifico e Tecnológico, and by Coordenação de Aperfeiçoamento de Pessoal de Nível Superior.

DISCLOSURES

No conflicts of interest, financial or otherwise, are declared by the author(s).

AUTHOR CONTRIBUTIONS

B.H.I., L.d.S., T.D.P., E.L.A., B.P.M.P., F.A.S., L.R.C.-L., P.J.F.T., G.M., and A.C.C.G. conception and design of research; B.H.I., L.d.S., T.D.P., E.L.A., B.P.M.P., F.A.S., L.R.C.-L., and G.M. performed experiments; B.H.I., L.d.S., T.D.P., E.L.A., B.P.M.P., F.A.S., L.R.C.-L., G.M., and A.C.C.G. analyzed data; B.H.I., L.d.S., T.D.P., E.L.A., G.M., and A.C.C.G. interpreted results of experiments; B.H.I., L.d.S., and A.C.C.G. prepared figures; B.H.I., L.d.S., T.D.P., E.L.A., B.P.M.P., F.A.S., L.R.C.-L., P.J.F.T., G.M., and A.C.C.G. edited and revised manuscript; B.H.I., L.d.S., T.D.P., E.L.A., B.P.M.P., F.A.S., L.R.C.-L., P.J.F.T., G.M., and A.C.C.G. approved final version of manuscript; A.C.C.G. drafted manuscript.

REFERENCES

1. **Abraham WT, Lowes BD, Ferguson DA, Odom J, Kim JK, Robertson AD, Bristow MR, Schrier RW.** Systemic hemodynamic, neurohormonal, and renal effects of a steady-state infusion of human brain natriuretic peptide in patients with hemodynamically decompensated heart failure. *J Card Fail* 4: 37–44, 1998.
2. **Antonio EL, Dos Santos AA, Araujo SR, Bocalini DS, Dos Santos L, Fenelon G, Franco MF, Tucci PJ.** Left ventricle radio-frequency ablation in the rat: a new model of heart failure due to myocardial infarction homogeneous in size and low in mortality. *J Card Fail* 15: 540–548, 2009.
3. **Aronson PS.** Energy-dependence of phlorizin binding to isolated renal microvillus membranes. Evidence concerning the mechanism of coupling between the electrochemical Na^+ gradient the sugar transport. *J Membr Biol* 42: 81–98, 1978.
4. **Biemesderfer D, Pizzonia J, Abu-Alfa A, Exner M, Reilly R, Igarashi P, Aronson PS.** NHE3: a Na^+/H^+ exchanger isoform of renal brush border. *Am J Physiol Renal Fluid Electrolyte Physiol* 265: F736–F742, 1993.
5. **Biemesderfer D, Rutherford PA, Nagy T, Pizzonia JH, Abu-Alfa AK, Aronson PS.** Monoclonal antibodies for high-resolution localization of NHE3 in adult and neonatal rat kidney. *Am J Physiol Renal Physiol* 273: F289–F299, 1997.
6. **Burnett JC Jr, Kao PC, Hu DC, Heser DW, Heublein D, Granger JP, Opgenorth TJ, and Reeder GS.** Atrial natriuretic peptide elevation in congestive heart failure in the human. *Science* 231: 1145–1147, 1986.
7. **Cadnapaphornchai MA, Gurevich AK, Weinberger HD, Schrier RW.** Pathophysiology of sodium and water retention in heart failure. *Cardiology* 96: 122–131, 2001.
8. **Chen HH, Schrier RW.** Pathophysiology of volume overload in acute heart failure syndromes. *Am J Med* 119: S11–S16, 2006.
9. **Cody RJ, Atlas SA, Laragh JH, Kubo SH, Covit AB, Ryman KS, Shaknovich A, Pondolfino K, Clark M, Camargo MJ.** Atrial natriuretic factor in normal subjects and heart failure patients Plasma levels and renal, hormonal, and hemodynamic responses to peptide infusion. *J Clin Invest* 78: 1362–1374, 1986.
10. **Crajoinas RO, Lessa LM, Carraro-Lacroix LR, Davel AP, Pacheco BP, Rossoni LV, Malnic G, Girardi AC.** Posttranslational mechanisms associated with reduced NHE3 activity in adult vs. young prehypertensive SHR. *Am J Physiol Renal Physiol* 299: F872–F881, 2010.
11. **Crajoinas RO, Oricchio FT, Pessoa TD, Pacheco BP, Lessa LM, Malnic G, Girardi AC.** Mechanisms mediating the diuretic and natriuretic actions of the incretin hormone glucagon-like peptide-1. *Am J Physiol Renal Physiol* 301: F355–F363, 2011.
12. **Davidson WD, Sackner MA.** Simplification of the anthrone method for the determination of inulin in clearance studies. *J Lab Clin Med* 62: 351–356, 1963.
13. **de Bold AJ, Bruneau BG, Kuroski de Bold ML.** Mechanical and neuroendocrine regulation of the endocrine heart. *Cardiovasc Res* 31: 7–18, 1996.
14. **Dixit MP, Xu L, Xu H, Bai L, Collins JF, Ghishan FK.** Effect of angiotensin-II on renal Na^+/H^+ exchanger-NHE3 and NHE2. *Biochim Biophys Acta* 1664: 38–44, 2004.
15. **Dynia DW, Steinmetz AG, Kocinsky HS.** NHE3 function and phosphorylation are regulated by a calyculin A-sensitive phosphatase. *Am J Physiol Renal Physiol* 298: F745–F753, 2010.
16. **Dzau VJ, Colucci WS, Hollenberg NK, Williams GH.** Relation of the renin-angiotensin-aldosterone system to clinical state in congestive heart failure. *Circulation* 63: 645–651, 1981.
17. **Eiskjaer H, Bagger JP, Danielsen H, Jensen JD, Jespersen B, Thomsen K, Sorensen SS, Pedersen EB.** Mechanisms of sodium retention in heart failure: relation to the renin-angiotensin-aldosterone system. *Am J Physiol Renal Fluid Electrolyte Physiol* 260: F883–F889, 1991.
18. **Fernandez-Llama P, Ageloff S, Fernandez-Varo G, Ros J, Wang X, Garra N, Esteva-Font C, Ballarin J, Barcelo P, Arroyo V, Stokes JB, Knepper MA, Jimenez W.** Sodium retention in cirrhotic rats is associated with increased renal abundance of sodium transporter proteins. *Kidney Int* 67: 622–630, 2005.
19. **Hall RA, Premont RT, Chow CW, Blitzer JT, Pitcher JA, Claing A, Stoffel RH, Barak LS, Shenolikar S, Weinman EJ, Grinstein S, Lefkowitz RJ.** The β_2-adrenergic receptor interacts with the Na^+/H^+-exchanger regulatory factor to control Na^+/H^+ exchange. *Nature* 392: 626–630, 1998.
20. **Harris PJ, Young JA.** Dose-dependent stimulation and inhibition of proximal tubular sodium reabsorption by angiotensin II in the rat kidney. *Pflügers Arch* 367: 295–297, 1977.
21. **Howard RL, Schrier RW.** A unifying hypothesis of sodium and water regulation in health and disease. *Horm Res* 34: 118–123, 1990.
22. **Jose PA, Eisner GM, Felder RA.** Dopamine and the kidney: a role in hypertension? *Curr Opin Nephrol Hypertens* 12: 189–194, 2003.
23. **Kocinsky HS, Dynia DW, Wang T, Aronson PS.** NHE3 phosphorylation at serines 552 and 605 does not directly affect NHE3 activity. *Am J Physiol Renal Physiol* 293: F212–F218, 2007.
24. **Kocinsky HS, Girardi AC, Biemesderfer D, Nguyen T, Mentone S, Orlowski J, Aronson PS.** Use of phospho-specific antibodies to determine the phosphorylation of endogenous Na^+/H^+ exchanger NHE3 at PKA consensus sites. *Am J Physiol Renal Physiol* 289: F249–F258, 2005.
25. **Kurashima K, Yu FH, Cabado AG, Szabo EZ, Grinstein S, Orlowski J.** Identification of sites required for down-regulation of Na^+/H^+ exchanger NHE3 activity by cAMP-dependent protein kinase phosphorylation-dependent and -independent mechanisms. *J Biol Chem* 272: 28672–28679, 1997.
26. **LaPointe MS, Sodhi C, Sahai A, Batlle D.** Na^+/H^+ exchange activity and NHE-3 expression in renal tubules from the spontaneously hypertensive rat. *Kidney Int* 62: 157–165, 2002.
27. **Lowry OH, Rosebrough NJ, Farr AL, Randall RJ.** Protein measurement with the Folin phenol reagent. *J Biol Chem* 193: 265–275, 1951.
28. **Lütken SC, Kim SW, Jonassen T, Marples D, Knepper MA, Kwon TH, Frokiaer J, Nielsen S.** Changes of renal AQP2, ENaC, and NHE3 in experimentally induced heart failure: response to angiotensin II AT1 receptor blockade. *Am J Physiol Renal Physiol* 297: F1678–F1688, 2009.
29. **McDonough AA.** Mechanisms of proximal tubule sodium transport regulation that link extracellular fluid volume and blood pressure. *Am J Physiol Regul Integr Comp Physiol* 298: R851–R861, 2010.
30. **Meneton P.** Comparative roles of the renal apical sodium transport systems in blood pressure control. *J Am Soc Nephrol* 11, *Suppl* 16: S135–S139, 2000.
31. **Nogae S, Michimata M, Kanazawa M, Honda S, Ohta M, Imai Y, Ito S, Matsubara M.** Cardiac infarcts increase sodium transporter transcripts (rBSC1) in the thick ascending limb of Henle. *Kidney Int* 57: 2055–2063, 2000.
32. **Omland T, Aakvaag A, Bonarjee VV, Caidahl K, Lie RT, Nilsen DW, Sundsfjord JA, Dickstein K.** Plasma brain natriuretic peptide as an indicator of left ventricular systolic function and long-term survival after acute myocardial infarction. Comparison with plasma atrial natriuretic peptide and N-terminal proatrial natriuretic peptide. *Circulation* 93: 1963–1969, 1996.

33. **Pedrosa R, Gomes P, Soares-da-Silva P.** Distinct signalling cascades downstream to Gs_{α} coupled dopamine D1-like NHE3 inhibition in rat and opossum renal epithelial cells. *Cell Physiol Biochem* 14: 91–100, 2004.
34. **Queiroz-Leite GD, Peruzzetto MC, Neri EA, Reboucas NA.** Transcriptional regulation of the Na/H exchanger NHE3 by chronic exposure to angiotensin II in renal epithelial cells. *Biochem Biophys Res Commun* 409: 470–476, 2011.
35. **Remes J.** Neuroendocrine activation after myocardial infarction. *Br Heart J* 72: S65–S69, 1994.
36. **Riegger GA, Kromer EP, Kochsiek K.** Human atrial natriuretic peptide: plasma levels, hemodynamic, hormonal, and renal effects in patients with severe congestive heart failure. *J Cardiovasc Pharmacol* 8: 1107–1112, 1986.
37. **Saccomani G, Mitchell KD, Navar LG.** Angiotensin II stimulation of Na^+-H^+ exchange in proximal tubule cells. *Am J Physiol Renal Fluid Electrolyte Physiol* 258: F1188–F1195, 1990.
38. **Schrier RW.** Body fluid volume regulation in health and disease: a unifying hypothesis. *Ann Intern Med* 113: 155–159, 1990.
39. **Schrier RW, Abraham WT.** Hormones and hemodynamics in heart failure. *N Engl J Med* 341: 577–585, 1999.
40. **Schultheis PJ, Clarke LL, Meneton P, Miller ML, Soleimani M, Gawenis LR, Riddle TM, Duffy JJ, Doetschman T, Wang T, Giebisch G, Aronson PS, Lorenz JN, Shull GE.** Renal and intestinal absorptive defects in mice lacking the NHE3 Na^+/H^+ exchanger. *Nat Genet* 19: 282–285, 1998.
41. **Schwark JR, Jansen HW, Lang HJ, Krick W, Burckhardt G, Hropot M.** S3226, a novel inhibitor of Na^+/H^+ exchanger subtype 3 in various cell types. *Pflügers Arch* 436: 797–800, 1998.
42. **Sonalker PA, Tofovic SP, Bastacky SI, Jackson EK.** Chronic noradrenaline increases renal expression of NHE-3, NBC-1, BSC-1 and aquaporin-2. *Clin Exp Pharmacol Physiol* 35: 594–600, 2008.
43. **Staahltoft D, Nielsen S, Janjua NR, Christensen S, Skott O, Marcussen N, Jonassen TE.** Losartan treatment normalizes renal sodium and water handling in rats with mild congestive heart failure. *Am J Physiol Renal Physiol* 282: F307–F315, 2002.
44. **Stead EA, Warren JV.** The protein content of the extracellular fluid in normal subjects after venous congestion and in patients with cardiac failure, anoxemia, and fever. *J Clin Invest* 23: 283–287, 1944.
45. **Thekkumkara T, Linas SL.** Role of internalization in AT_{1A} receptor function in proximal tubule epithelium. *Am J Physiol Renal Physiol* 282: F623–F629, 2002.
46. **Thomas D, Harris PJ, Morgan TO.** Age-related changes in angiotensin II-stimulated proximal tubule fluid reabsorption in the spontaneously hypertensive rat. *J Hypertens Suppl* 6: S449–S451, 1988.
47. **Tomoda H.** Atrial natriuretic peptide in acute myocardial infarction. *Am J Cardiol* 62: 1122–1123, 1988.
48. **Torp M, Brond L, Hadrup N, Nielsen JB, Praetorius J, Nielsen S, Christensen S, Jonassen TE.** Losartan decreases vasopressin-mediated cAMP accumulation in the thick ascending limb of the loop of Henle in rats with congestive heart failure. *Acta Physiol (Oxf)* 190: 339–350, 2007.
49. **Tsuganezawa H, Preisig PA, Alpern RJ.** Dominant negative c-Src inhibits angiotensin II induced activation of NHE3 in OKP cells. *Kidney Int* 54: 394–398, 1998.
50. **Turban S, Beutler KT, Morris RG, Masilamani S, Fenton RA, Knepper MA, Packer RK.** Long-term regulation of proximal tubule acid-base transporter abundance by angiotensin II. *Kidney Int* 70: 660–668, 2006.
51. **Vallon V, Schwark JR, Richter K, Hropot M.** Role of Na^+/H^+ exchanger NHE3 in nephron function: micropuncture studies with S3226, an inhibitor of NHE3. *Am J Physiol Renal Physiol* 278: F375–F379, 2000.
52. **Wang T, Hropot M, Aronson PS, Giebisch G.** Role of NHE isoforms in mediating bicarbonate reabsorption along the nephron. *Am J Physiol Renal Physiol* 281: F1117–F1122, 2001.
53. **Woods RL.** Cardioprotective functions of atrial natriuretic peptide and B-type natriuretic peptide: a brief review. *Clin Exp Pharmacol Physiol* 31: 791–794, 2004.
54. **Xu L, Dixit MP, Nullmeyer KD, Xu H, Kiela PR, Lynch RM, Ghishan FK.** Regulation of Na^+/H^+ exchanger-NHE3 by angiotensin-II in OKP cells. *Biochim Biophys Acta* 1758: 519–526, 2006.
55. **Yang LE, Leong PK, Ye S, Campese VM, McDonough AA.** Responses of proximal tubule sodium transporters to acute injury-induced hypertension. *Am J Physiol Renal Physiol* 284: F313–F322, 2003.
56. **Yoshimura M, Yasue H, Okumura K, Ogawa H, Jougasaki M, Mukoyama M, Nakao K, Imura H.** Different secretion patterns of atrial natriuretic peptide and brain natriuretic peptide in patients with congestive heart failure. *Circulation* 87: 464–469, 1993.